Path Planning for Planetary Exploration Rovers and Its Evaluation based on Wheel Slip Dynamics

Genya Ishigami, Keiji Nagatani, and Kazuya Yoshida

Abstract— **In this paper, a path planning and its evaluation method is described with taking into account wheel slip dynamics of lunar/planetary exploration rovers. The surface of the planetary body is largely covered with powdery soil. On such loose soil, the wheel slippage which will make the rover get stuck must be concerned. Since the slippage dynamically depends on the posture/velocity of vehicle, soil characteristics, and wheel-soil interactions, it becomes difficult issues to incorporate the wheel slip dynamics as a criterion into path-planning algorithms. To tackle the slippage problem, the authors develop the path-planning algorithm and the path-evaluation method based on the following approach. First, a path on a rough terrain is generated with the terrain-based criteria function. Subsequently, the dynamics simulation of a rover is carried out in which the rover is controlled to follow the candidate path. Finally, the path is properly evaluated based on the slip motion profiles calculated by the simulation. Demonstrations for the proposed technique are addressed along with a discussion on characteristics of the candidate path and the slip motion profile of the rover.**

I. Introduction

Substantial progresses in space exploration technology have significantly enabled us to perform various scientific missions, such as investigations about the origin of the solar system and the future in-situ resource utilization. The surface mobility by using wheeled mobile robots (*Rovers*) is one of the important technologies to expand exploration areas and deliver the in-situ devices to specific locations. The surface terrain of the Moon or a planet such as Mars is covered with fine-grained soil, boulders, rocks, or stones. Because of the challenging terrain, the rover must design an appropriate path to avoid mobility hazards such as wheel-stuck, vehicle tip-over, and collision with obstacles.

There are a great number of papers and books regarding path/motion planning issues [1]-[6]. For example, a dynamic motion planning considering constrains on vehicle motions has been investigated in [2]. A general constrained optimization approach for trajectory generation has also been proposed in [4]. Further, a planning algorithm with model-based evaluations, that include uncertainties of the terrain measurement and rover localization, has been developed in [5]. Despite such intensive research, the vehicle dynamics or slip motion have not been sufficiently addressed in the planning issues. The slip motion is easily generated when the rover travels on loose terrain even if the general cruising velocity of the rover is relatively slow. Therefore, it becomes difficult issues to include the slip dynamics as criteria of the path-planning algorithms since such slip motion dynamically depends on the posture of the vehicle, velocity of the wheel, and soil characteristics.

The mechanics of the slipping wheel on loose soil has been studied in the field of *terramechanics* [7]-[10]. In this field, the principle of the wheel-soil interaction mechanics and the modeling of the stress distributions beneath the wheels have been previously investigated [7][8]. We have also elaborated upon the wheel-and-vehicle model to analyze the motion maneuver of the rover [9][10].

In this paper, a path planning algorithm and its evaluation method are addressed by applying our background regarding the wheel slip dynamics. Our approach consists of three steps; 1) the path planning to derive a candidate path, 2) the dynamics simulation in which the rover is controlled to follow the candidate path, and 3) the path evaluation based on the dynamic simulation results. Demonstrations for the path planning and evaluation using the proposed technique are also described in this paper. The result indicates that it is able to generate a reasonable path and quantitatively evaluate candidate path using the proposed technique.

The paper is organized as follows. Section II describes an outline of the proposed technique for the path planning and evaluation method. In Section III, the path-planning algorithm is introduced. The dynamics simulation model and the path following strategy for the path evaluation method are presented in Section IV and Section V, respectively. In Section VI, the simulation study and performance of the proposed technique are described.

II. Outline of Path Planning and Evaluation Method

Fig. 1 shows a flow chart of the proposed technique for the path planning and evaluation method. As mentioned in Section I, our approach consists of the following three steps.

In the first step, the path-planning problem is addressed as an extended shortest path problem, and then, a candidate path on a given terrain map is obtained by using the Dijkstra's algorithm [6].

As the second step, in order to calculate motion profiles of the rover, the dynamics simulation of a rover is carried out in which the rover is controlled to follow the candidate path. The dynamic behavior of the rover is modeled based on the wheel-and-vehicle model, which has been developed and validated in our previous researches [9][10]. The interaction of wheel on loose soil is properly addressed based on the terramechanics approach. Here, it is possible to discuss the

This work was supported in part by Research Fellowships of the Japan Society for the Promotion of Science for Young Scientists.

The authors are with Department of Aerospace Engineering, Tohoku University, Aoba 6-6-01, Sendai, 980-8579, Japan, {ishigami,keiji,yoshida}@astro.mech.tohoku.ac.jp

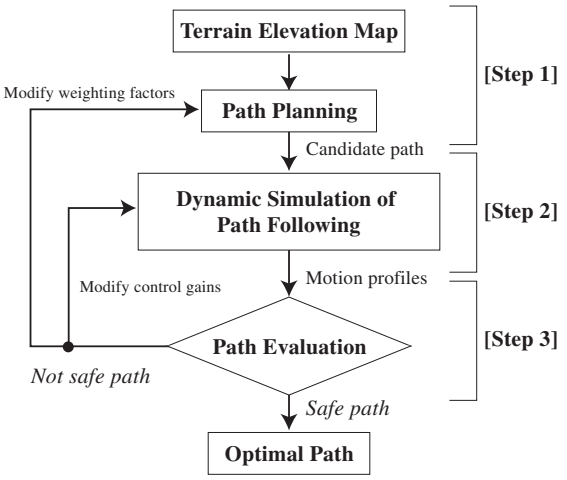

Fig. 1. Flow chart of the path planning algorithm and evaluation method

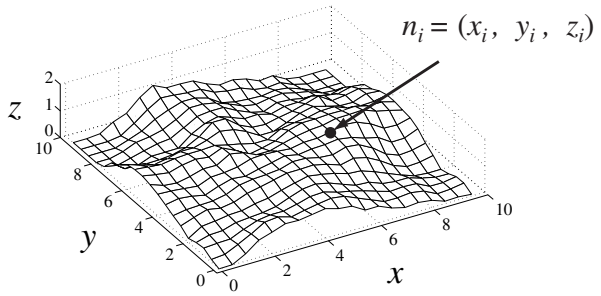

Fig. 2. Terrain map example (DEM 50×50 nodes)

path-following error since the rover might not accurately follow the candidate path on challenging terrains.

In the third step, the candidate path is properly evaluated based on the results of the dynamic simulation. The criteria of the path evaluation are determined as wheel slippages, vehicle postures and elapsed time/total travel distance from the initial point to the destination of the path.

III. Path Planning Algorithm

In this path planning issue, it is assumed that a terrain map where a rover travels has been already given without any uncertainties. As shown in Fig. 2, the terrain map is represented as Digital Elevation Map (DEM) which is defined by a series of elevations along with a node n_i in (x_i, y_i, z_i). Subscript i means a node number. It is generally known that such DEM-based terrain map can be easily measured and developed by using a Laser Range Finder (LRF) or stereo camera systems mounted on a rover in practical situation.

A. Criteria Index

A criteria function to find a candidate path is composed of three indexes: terrain roughness, path length and terrain inclination.

1) Terrain roughness index: The terrain roughness index is employed in order to make a rover avoid to traverse through uneven bumpy areas where obstacles, such as stones, rocks, and boulders, are spread over.

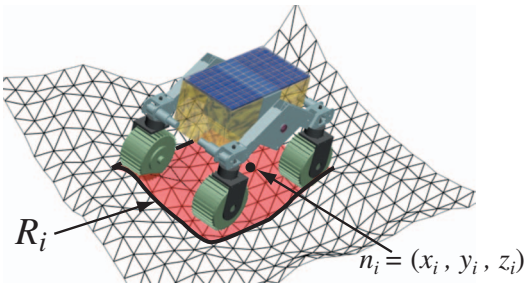

Fig. 3. Projection region of a rover on terrain

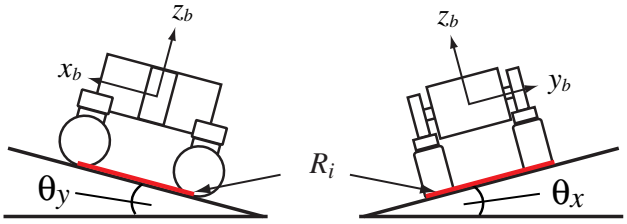

Fig. 4. Terrain inclination angles

The terrain roughness index B_i is given as a standard deviation of the terrain elevation over a projection region of a rover R_i [5]:

$$B_i = \sqrt{\frac{1}{n}\sum_{R_i}\left(z(R_i) - \bar{z}(R_i)\right)^2} \tag{1}$$

As shown in Fig. 3, the projection region R_i includes the set of terrain elevation points inside the region surrounded by wheels. In the above equation, n represents a number of nodes inside the region and $\bar{z}(R_i)$ denotes an average elevation in the R_i. The rougher the terrain is, the larger the value of B_i becomes.

2) Path length index: The path length index performs to find the shortest path from an initial point to a destination. The path length index L_i between adjacent nodes is simply calculated by the following equation:

$$L_i = |n_i - n_j| = \sqrt{(x_i - x_j)^2 + (y_i - y_j)^2 + (z_i - z_j)^2} \tag{2}$$

If the node n_j are not adjacent to the node n_i, L_i takes large enough value.

3) Terrain inclination index: When a rover climbs up a hill or traverses a slope of crater, risks of wheel slippage become larger since the traction load of the rover increases on slope situations. The index for the terrain inclination is employed in order to mitigate such risks. Terrain inclination angles are divided into two axes in accordance with the rover coordinate as described in Fig. 4. An inclination angle around x-axis of the rover coordinate is denoted by θ_x, while the one around y-axis is θ_y. The indexes, Θ_{xi} and Θ_{y_i}, associated with each terrain inclination are respectively determined by the average inclination at the region R_i:

$$\Theta_{xi} = \bar{\theta}_x(R_i) \tag{3}$$

$$\Theta_{y_i} = \bar{\theta}_y(R_i) \tag{4}$$

The indexes for the terrain inclinations also indicate a hazard of vehicle tip-over since the roll and pitch angle of the vehicle are directly changed along with the terrain inclination.

B. Criteria Function for Candidate Path

Using the above indexes, the criteria function $C(\boldsymbol{p})$ to obtain a candidate path $\boldsymbol{p}$ is defined as follows:

$$C(\boldsymbol{p}) = \sum_{i=\boldsymbol{p}} \Big(W_B N_B B_i + W_L N_L L_i + W_{\theta_x} N_{\theta_x} \Theta_{x i} + W_{\theta_y} N_{\theta_y} \Theta_{y_i} \Big) \quad (5)$$

where, W_B, W_L, W_{θ_x}, and W_{θ_y} are weighting factors to give specific priorities between the terrain roughness, path length, and terrain inclinations. Note that, W_{θ_x} or W_{θ_y} respectively take large enough values when the index Θ_{xi} or Θ_{y_i} exceed threshold angles, $\theta_{x max}$ and $\theta_{y_{max}}$. N_B, N_L, N_{θ_x}, and N_{θ_y} are constant to make each corresponding index normalize and eliminate the dimensions. The path $\boldsymbol{p}$ consists of a series of neighboring nodes, $\boldsymbol{p} = \{n_{\text{start}}, \ \ldots, \ n_i, \ \ldots, \ n_{\text{goal}}\}$.

The smaller each value of the index is, the less the hazard at the path becomes. Therefore, by supposing the criteria function as a hypothetical distance function, the path-planning problem is considered as a shortest path search problem. Considering that the minimum criteria function derives the "shortest" path $\boldsymbol{p}_s$, the following equation can be formed:

$$\min C(\boldsymbol{p}) = C(\boldsymbol{p}_s) \quad (6)$$

In this research, the conventional Dijkstra's algorithm is employed [6] to derive the path $\boldsymbol{p}_s$.

IV. Dynamics Simulation Model for Path Evaluation

In the dynamics simulation for the path evaluation, the dynamic behavior of a rover is modeled with a wheel-and-vehicle model, which consists of two models: the vehicle dynamics model and the wheel-soil contact model. The wheel-and-vehicle dynamics model has been successfully developed and validated in our previous researches [9][10]. In particular, the interaction of wheel on loose soil is properly addressed based on the terramechanics approach.

A. Vehicle Dynamics Model

The vehicle in the simulation is referred to our rover test bed as shown in Fig. 5. The 4-wheeled rover test bed weighs about 35 [kg] in total. The rover has 0.48 [m] in the wheelbase and 0.34 [m] in tread. Each wheel of the rover has active steering and driving axles.

The dynamic motion of the rover for given traveling and steering conditions are numerically obtained by successively solving the following motion equation:

$$\boldsymbol{H} \begin{bmatrix} \dot{\boldsymbol{v}}_0 \\ \dot{\boldsymbol{\omega}}_0 \\ \ddot{\boldsymbol{q}} \end{bmatrix} + \boldsymbol{C} + \boldsymbol{G} = \begin{bmatrix} \boldsymbol{F}_0 \\ \boldsymbol{N}_0 \\ \boldsymbol{\tau} \end{bmatrix} + \boldsymbol{J}^T \begin{bmatrix} \boldsymbol{F}_e \\ \boldsymbol{N}_e \end{bmatrix} \quad (7)$$

where $\boldsymbol{H}$ represents the inertia matrix of the rover; $\boldsymbol{C}$, the velocity depending term; $\boldsymbol{G}$, the gravity term; $\boldsymbol{v}_0$ and $\boldsymbol{\omega}_0$, the translational velocity and angular velocity of the main body; $\boldsymbol{q}$, the angle of each joint of the rover; $\boldsymbol{F}_0$ and $\boldsymbol{N}_0$, the external forces and moments acting at the centroid of the main body; $\boldsymbol{\tau}$, the torques acting at each joint of the rover; $\boldsymbol{J}$, the Jacobian matrix; $\boldsymbol{F}_e = [f_{w1}, \ldots, f_{wm}]$, the external forces acting at the centroid of each wheel; $\boldsymbol{N}_e$, the external moments acting at the centroid of each wheel.

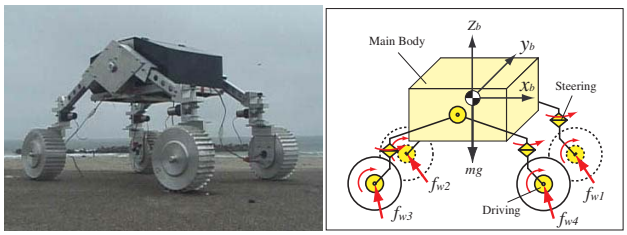

(Rover test bed) (Vehicle dynamics model)

Fig. 5. Rover test bed and vehicle dynamics model

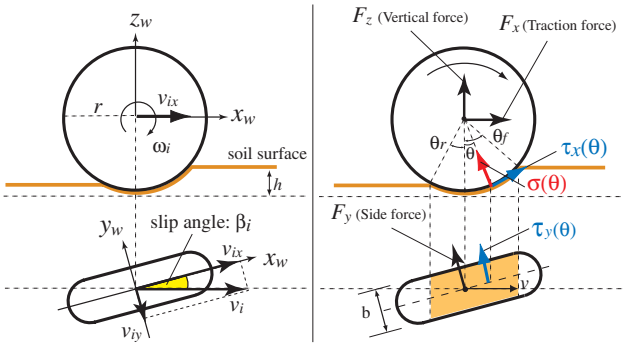

Fig. 6. Wheel-soil contact model

Each external force $\boldsymbol{f}_{wi}$ is calculated by the wheel-soil contact model, as mentioned in (10)-(12) later. The subscript i denotes the number of wheels (in this case, i=1, ..., 4).

The vehicle dynamics model, as illustrated in Fig. 5, has to be completely equivalent to the rover test bed. Specific parameters for the rover kinematics and dynamics are determined from the test bed and used in the simulation.

B. Wheel-Soil Contact Model

A general force model for a rigid wheel traveling on loose soil is shown in Fig. 6. A wheel coordinate system is defined as a right-hand frame; in this system the longitudinal direction is denoted by x_w, the lateral direction by y_w, and the vertical direction by z_w.

1) Wheel slippage: Wheel slippage can be measured by *slip ratio* and *slip angle*. The slip in the longitudinal direction is expressed by the slip ratio s_i, which is defined as a function of the longitudinal traveling velocity of the wheel v_{i_x} and the circumference velocity of the wheel $r\omega_i$:

$$s_i = \begin{cases} (r\omega_i - v_{i_x})/r\omega_i & (|r\omega_i| \geq |v_{i_x}| : \text{driving}) \\ (r\omega_i - v_{i_x})/v_{i_x} & (|r\omega_i| < |v_{i_x}| : \text{braking}) \end{cases} \quad (8)$$

where, r denotes the wheel radius. The slip ratio assumes a value in the range from -1.0 and 1.0.

On the other hand, the slip in the lateral direction is expressed by the slip angle β_i, which is defined by using

v_{i_x} and the lateral traveling velocity v_{i_y} as follows:

$$\beta_i = \tan^{-1}(v_{i_y}/v_{i_x}) \tag{9}$$

Typical techniques to measure these slips are, for example, to use an accelerometer or an IMU (Inertial Measurement Unit) as internal sensors, and also an RTK-GPS (Real Time Kinematic-GPS), or an LMS (Laser Measurement System) as external sensors.

2) Wheel contact forces: Based on the terramechanics approach, the wheel contact forces, such as the drawbar pull F_x, side force F_y, and vertical force F_z, can be obtained in the same fashion [8][9]:

$$F_x = rb\int_{\theta_r}^{\theta_f}\big(\tau_x(\theta)\cos\theta - \sigma(\theta)\sin\theta\big)d\theta \tag{10}$$

$$F_y = \int_{\theta_r}^{\theta_f}\big(rb\cdot\tau_y(\theta) + R_b\cdot(r - h(\theta)\cos\theta\big)d\theta \tag{11}$$

$$F_z = rb\int_{\theta_r}^{\theta_f}\big(\tau_x(\theta)\sin\theta + \sigma(\theta)\cos\theta\big)d\theta \tag{12}$$

where, b represents a width of the wheel; $\sigma(\theta)$, the normal stress beneath the wheel; $\tau_x(\theta)$ and $\tau_y(\theta)$, the shear stresses in the longitudinal and lateral direction of the wheel. The contact region of the wheel on loose soil is determined by the entry angle θ_f and the exit angle θ_r. In addition, R_b is modeled as a reaction resistance generated by the bulldozing phenomenon on a side face of the wheel [9]. R_b is given as a function of a wheel sinkage h.

Note that, σ, τ_x, and τ_y, that are the key components to derive the wheel forces, depends on the wheel slippage. The contact region of the wheel is also dominated by the slip behavior of wheel. Thus, the wheel-soil contact model can accurately explain the slipping wheel. The contact model has been successfully verified in [9].

V. Path Following Strategy

Path following strategy is shortly described to make the rover travel along with the candidate path. The strategy is referred to our previous research in [11] which takes into account slip motions. Based on the strategy, both steering and driving maneuvers of the rover are derived not only to follow an arbitrary path but also simultaneously compensate for the slip.

A. Path Following Control

A general illustration of the path following problem is shown in Fig. 7. The current vehicle's position is denoted by P, the shortest distance projection of P to a candidate path is denoted by P_d. Each symbol used in the path following problem is defined as follows: l_e represents the signed distance between P and P_d (distance error); θ_d, the angle between the x-axis and the tangent to the path at P_d (vehicle's desired orientation); θ_e, the orientation error $(\theta_0 - \theta_d)$; β_0, the sideslip of the vehicle.

In the path following problem, a feedback control law is employed to satisfy both $l_e \to 0$ and $\theta_e \to 0$. In addition, on loose soil, a vehicle has a certain amount of sideslip which must lead to an unexpected orientation error. This sideslip can be reduced by another control objective, namely $\beta_0 \to 0$. We consider that these control objectives are realized by the use of one control variable, which is a turning angular velocity of the vehicle $\omega_0(\dot{\theta}_0)$.

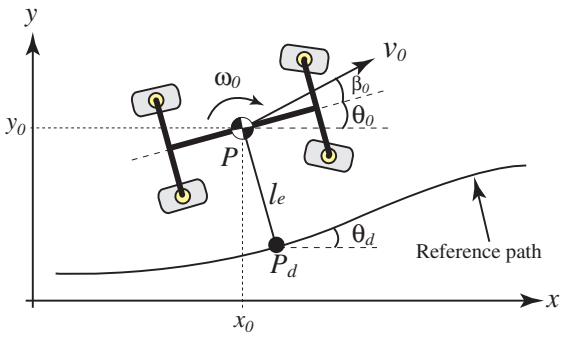

Fig. 7. Illustration of path following control

B. Steering and Driving Maneuvers with Slip Compensation

The path following control has to be realized by several actuators that are mainly located on steering and driving units.

1) Steering maneuvers: A desired steering angle of each wheel δ_{di} is elaborated upon by the following equation:

$$\delta_{di} = \tan^{-1}\left(\frac{v_d\sin\theta_d - \dot{Y}_i(\dot{\theta}_d)}{v_d\cos\theta_d - \dot{X}_i(\dot{\theta}_d)}\right) - \theta_d - \beta_i \tag{13}$$

where, v_d represents a desired linear velocity of the vehicle; X_i and Y_i, the distances between every wheel and the center of gravity of the vehicle. The procedure to obtain the desired turning angular velocity of vehicle $\dot{\theta}_d$ is referred to [11].

2) Driving maneuvers: The driving maneuver is defined as a control of wheel angular velocity. A desired wheel angular velocity ω_{di} is calculated by the following:

$$\omega_{di} = \begin{cases} \big(v_d\cos\theta_d + \dot{X}_i(\dot{\theta}_d)\big)\cdot\cos\beta_i/r\cos\phi_i & (\theta_d \le \pi/4) \\ \big(v_d\sin\theta_d + \dot{Y}_i(\dot{\theta}_d)\big)\cdot\cos\beta_i/r\sin\phi_i & (\theta_d \ge \pi/4) \end{cases} \tag{14}$$

where, $\phi_i = \theta_0 + \delta_i + \beta_i$.

The desired wheel angular velocity has to be adjusted to compensate the longitudinal slip of wheel. Therefore, an improved desired angular velocity $\hat{\omega}_{di}$ compensating the longitudinal slip is rewritten as follows:

$$\hat{\omega}_{di} = \omega_{di}/\big(1 - (s_{ref} - s_i)\big) \tag{15}$$

where, s_{ref} means a reference slip ratio to regulate the longitudinal slip of wheel. In our approach, the value of s_{ref} is given between 0.1 and 0.3, where a wheel traction is obtained the most efficient value referring to our previous researches.

VI. Simulation of Path Planning and Evaluation

The path planning and evaluation simulation was conducted along with comparisons of two candidate paths. Each path is evaluated based on the wheel slippage, vehicle posture and elapsed time/total travel distance from the initial point to the destination of the path.

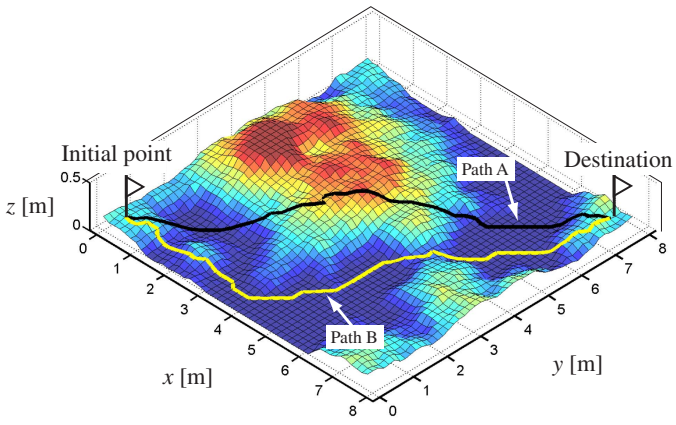

Fig. 8. Illustration of terrain elevation map and planned paths

A. Simulation procedure

The procedure of the path planning and evaluation simulation is summarized as follows:

1) Input the terrain elevation map to the path planning algorithm.
2) Determine the weighting factors and thresholds for terrain inclinations and then input them into (5).
3) Find the candidate path $\boldsymbol{p}_s$ based on (6).
4) The candidate path is incorporated into the dynamics simulation for the path following.
5) Derive the path following maneuvers, δ_{di} and $\hat{\omega}_{di}$, based on (13) and (15).
6) Calculate the external forces $\boldsymbol{f}_{wi}$ acting to each wheel using the wheel-soil contact model ((10)-(12)).
7) Determine $\boldsymbol{F}_0$, $\boldsymbol{N}_0$, $\boldsymbol{F}_e$, $\boldsymbol{N}_e$, and $\boldsymbol{\tau}$.
8) Solve (7), then obtain the rover position, orientation and velocity.
9) Calculate the sideslip of the rover, slip ratios and slip angles of each wheel, then return to the step 5) until the rover arrivers at the destination of $\boldsymbol{p}_s$.
10) Finally, the path is evaluated based on the motion profile obtained by the dynamics simulation.

B. Terrain Elevation Map

As shown in Fig. 8, the terrain elevation map is 8 [m] $\times$ 8 [m] square with a grid of 50 $\times$ 50 equally-spaced terrain nodes (total nodes in the map are 2500.) The elevation map is obtained by the fractal method as presented in [12]. In the simulation, the surface is supposed to be evenly covered with the *lunar regolith simulant*, which is simulated lunar surface soil in terms of similar material components and mechanical characteristics [13].

C. Path Planning

We carried out the simulation along with two candidate paths, path A and path B, generated by changing thresholds for terrain inclinations. The weighting factors and thresholds to obtain these two paths are summarized in Table I.

The candidate paths are depicted in Fig. 8. The values of the path characteristics, such as the total length and inclinations of the path, are summarized in Table II.

TABLE I

WEIGHTING FACTORS AND THRESHOLDS

Path	W_B	W_D	W_{θ_x}	W_{θ_y}	$\theta_{x\,max}$ [deg]	$\theta_{y\,max}$ [deg]
Path A	0.3	0.3	0.2	0.2	15.0	15.0
Path B	0.3	0.3	0.2	0.2	7.5	7.5

TABLE II

CHARACTERISTICS OF PLANNED PATHS

Path	Total length [m]	Inclinations [deg]			
		Maximum		Deviation	
		θ_x	θ_y	θ_x	θ_y
Path A	10.60	12.37	9.67	5.17	4.26
Path B	12.42	5.93	7.49	2.34	2.63

TABLE III

PATH EVALUATION RESULTS

Path	Elapsed time [sec]	Slip ratio (RMS)	Slip angle (RMS) [deg]
Path A	175.0	0.08	2.37
Path B	197.5	0.08	1.19

It can be seen that path A is generated as making the path directly from the initial point to the destination, while path B is planned to avoid a hill located around the center of the map. This difference between the candidate paths is due to the difference of the threshold for terrain inclinations. The characteristics of each path can be deduced as follows: path A is relatively short path, but implies hazards of the wheel slippage or the instability of the vehicle. Path B is expected to be a hazard less path, but it will take longer time to reach the destination.

D. Path Evaluation and Discussion

As described above, two paths are evaluated using motion profiles obtained by the dynamics simulations.

Time profiles of the vehicle orientations (roll and pitch angles), slip ratios, and slip angles of each wheel are shown in Fig. 9, Fig. 10, and Fig. 11, respectively. The dynamic motion of the rover on each path is illustrated in Fig. 12. The path evaluation results are listed in Table III. Here, the values of the slip ratio and slip angle are evaluated by employing root mean square (RMS), respectively.

From the figures and the table, first, it can be clearly seen that the vehicle orientation on path A is less stable (around $\pm 10^\circ$ fluctuation) as compared to that of path B. This is because the terrain inclination in path A is rougher than that in path B, and also, this result indicates that path A might have a hazard of the tip over.

Interestingly, however, there are few differences in slip ratio of wheels on both paths. The result in slip ratio conflicts with the one in the vehicle orientation, however, this is probably due to the path following control with slip compensation.

According to Fig. 11 and Table III, the deviation of slip angle on path A is almost twice as large as the that of path B. This can be explained that the large fluctuations of slip angle on path A, which is particularly observed from 80 [sec] to 120 [sec] in Fig. 11, is caused by the hill placed around the center of the map.

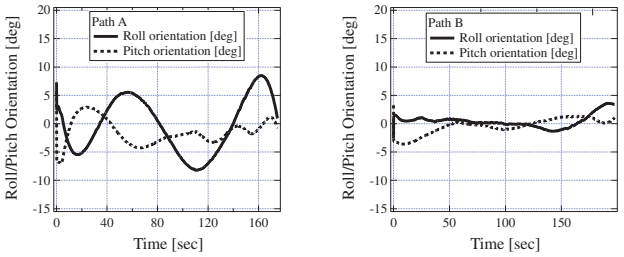

Fig. 9. Simulation result : time profile of vehicle orientation

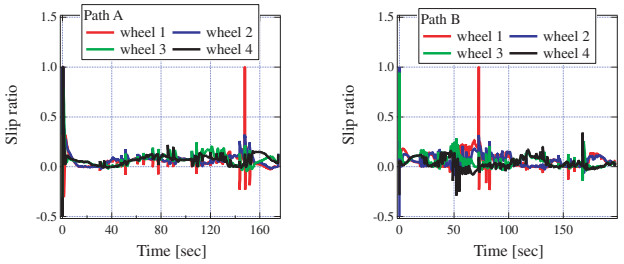

Fig. 10. Simulation result : time profile of slip ratio

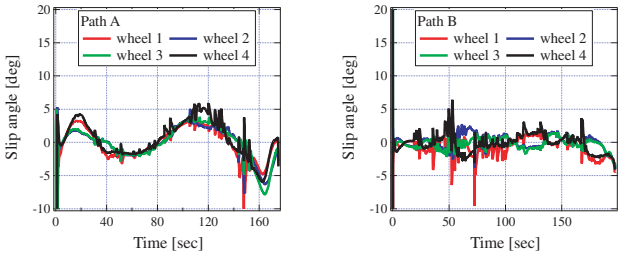

Fig. 11. Simulation result : time profile of slip angle

VII. Conclusion and Future Works

In this paper, the path planning and its evaluation method for lunar/planetary exploration rovers has been addressed with considering the wheel slip dynamics. The proposed technique has been composed of three steps; 1) the path planning to derive a candidate path, 2) the dynamics simulation in which the rover is controlled to follow the candidate path, and 3) the path evaluation based on the dynamic simulation results

The demonstration for the proposed technique has been described through a comparison between two different paths. The candidate path has been reasonably generated based on the path-planning algorithm. Further, the result shows that the proposed technique is able to quantitatively evaluate and discuss slip less, hazard less, and the safest path.

The proposed technique can also be applied to more scenarios, such as boulder/rocky fields or crater walls, by incorporating the corresponding terrain map into the path-planning algorithm. It is also expected to avoid the mobility hazard including wheel-stuck or vehicle tip-over based on the preliminarily evaluation of a candidate path in practical situations.

In the step of the path planning, the weighting factors were given constant values; however, it will be necessary to dynamically adjust these values in order to find more reasonable path in accordance with vehicle/terrain conditions.

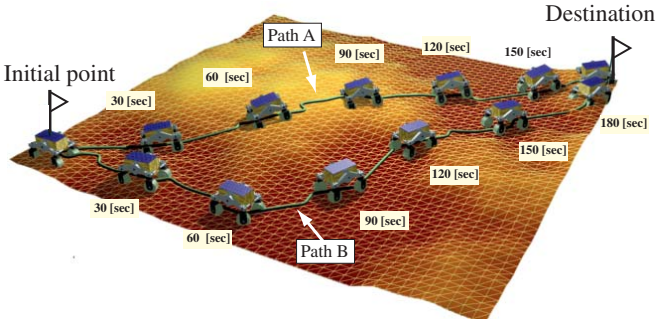

Fig. 12. Illustration of path evaluation simulation

The terrain characteristics and soil parameters should be included in the path planning criteria since the surface of the planetary body consists of different types of soft soil and hard rocks/stones.

As described in this paper, we have focused on the preliminary analysis of the traversing performance of rover on a given terrain map. To apply the proposed technique to an onboard usage, the following issues should be addressed: as for the path-planning algorithm, it is needed to simplify/improve the path searching method in order to derive a candidate path more efficiently and quickly. In addition, although it is assumed that all soil parameters are already known in our simulation, in-situ measurements of these parameters by using soil measurement devices should be considered in practical situation.

References

[1] A. De Luca, G. Oriolo, and C. Samson; *Robot Motion Planning and Control*, edtied by J.-P Laumond, Springer-Verlag, 1998.

[2] Z. Shiller and Y. R. Gwo; "Dynamic Motion Planning of Autonomous Vehicles," *IEEE Trans. on Robotics And Automation,* vol. 7, no. 2, pp. 241-249, April 1991.

[3] T. Kubota et al., "Path Planning for Newly Developed Microrover," *Proc. of the 2001 IEEE Int. Conf. on Robotics And Automation,* pp. 3710-3715, 2001.

[4] T. M. Howard and A. Kelly; "Terrain-Adaptive Generation of Optimal Continuous Trajectories for Mobile Robots," *Proc. of the 8th Int. Symp. on Artificial Intelligence, Robotics and Automation in Space*, 2005.

[5] K. Iagnemma and S. Dubowsky; *Mobile Robot in Rough Terrain*, Springer Tracts in Advanced Robotics, vol.12, 2004.

[6] Steven M. LaValle; *PLANNING ALGORITHMS*, Cambridge University Press, 2006.

[7] M. G. Bekker; *Introduction to Terrain-Vehicle Systems*, The University of Michigan Press, 1969.

[8] J. Y. Wong; *Theory of Ground Vehicles*, John Wiley & Sons, 1978.

[9] G. Ishigami and K. Yoshida; "Steering Characteristics of an Exploration Rover on Loose Soil Based on All-Wheel Dynamics Model," *Proc. of the 2005 IEEE Int. Conf. on Intelligent Robots and Systems,* pp. 2041-2046, 2005.

[10] G. Ishigami, A. Miwa, and K. Yoshida; "Steering Trajectory Analysis of Planetary Exploration Rovers Based on All-Wheel Dynamics Model," *Proc. of the 8th Int. Symp. on Artificial Intelligence, Robotics and Automation in Space*, 2005.

[11] G. Ishigami, K. Nagatani, and K. Yoshida; "Path Following Control with Slip Compensation on Loose Soil for Exploration Rover," *Proc. of the 2006 IEEE Int. Conf. on Intelligent Robots and Systems,*, pp. 5552-5557, 2006.

[12] Y. Yokokoji, S. Chaen, and T. Yoshikawa; "Evaluation of Traversability of Wheeled Mobile Robots on Uneven Terrains by Fractal Terrain Model," *Proc. of the 2004 IEEE Int. Conf. on Robotics And Automation,* pp. 2183-2188, 2004.

[13] H. Kanamori et al., "Properties of lunar soil simulant manufactured in Japan," *Proc. of the 6th Int. Conf. and Exposition on Engineering, Construction, and Operations in Space*, 1998.